Lecture Notes in Civil Engineering

Shashi Mesapam
Anurag Ohri
Venkataramana Sridhar
Nitin Kumar Tripathi *Editors*

Developments and Applications of Geomatics

Proceedings of DEVA 2022

Springer

Lecture Notes in Civil Engineering

Volume 450

Lecture Notes in Civil Engineering (LNCE) publishes the latest developments in Civil Engineering—quickly, informally and in top quality. Though original research reported in proceedings and post-proceedings represents the core of LNCE, edited volumes of exceptionally high quality and interest may also be considered for publication. Volumes published in LNCE embrace all aspects and subfields of, as well as new challenges in, Civil Engineering. Topics in the series include:

- Construction and Structural Mechanics
- Building Materials
- Concrete, Steel and Timber Structures
- Geotechnical Engineering
- Earthquake Engineering
- Coastal Engineering
- Ocean and Offshore Engineering; Ships and Floating Structures
- Hydraulics, Hydrology and Water Resources Engineering
- Environmental Engineering and Sustainability
- Structural Health and Monitoring
- Surveying and Geographical Information Systems
- Indoor Environments
- Transportation and Traffic
- Risk Analysis
- Safety and Security

To submit a proposal or request further information, please contact the appropriate Springer Editor:

- Pierpaolo Riva at pierpaolo.riva@springer.com (Europe and Americas);
- Swati Meherishi at swati.meherishi@springer.com (Asia—except China, Australia, and New Zealand);
- Wayne Hu at wayne.hu@springer.com (China).

All books in the series now indexed by Scopus and EI Compendex database!

Shashi Mesapam · Anurag Ohri ·
Venkataramana Sridhar · Nitin Kumar Tripathi
Editors

Developments and Applications of Geomatics

Proceedings of DEVA 2022

Springer

Editors
Shashi Mesapam
Department of Civil Engineering
National Institute of Technology Warangal
Hanamkonda, Telangana, India

Venkataramana Sridhar
Department of Biological Systems Engineering
Virginia Tech
Blacksburg, VA, USA

Anurag Ohri
Department of Civil Engineering
Indian Institute of Technology (Banaras Hindu University)
Varanasi, India

Nitin Kumar Tripathi
School of Engineering and Technology
Asian Institute of Technology
Bangkok, Thailand

ISSN 2366-2557 ISSN 2366-2565 (electronic)
Lecture Notes in Civil Engineering
ISBN 978-981-99-8567-8 ISBN 978-981-99-8568-5 (eBook)
https://doi.org/10.1007/978-981-99-8568-5

This Springer imprint is published by the registered company Springer Nature Singapore Pte Ltd.
The registered company address is: 152 Beach Road, #21-01/04 Gateway East, Singapore 189721, Singapore

Foreword

It gives me immense pleasure to write this foreword to the "Lecture notes in Civil Engineering" containing the selected papers presented during the International Virtual Conference on Developments and Applications of Geomatics (DEVA—2022) held during 29th–31st August, 2022. The conference was held to coincide with the superannuation of Prof. Deva Pratap.

NITW has been running an M.Tech. course in Remote Sensing and GIS, in the Department of Civil Engineering, since 2000 and has established itself as a pioneering institute in the field with its alumni occupying key positions. Many Ph.D. level research work and sponsored R&D works are in progress.

I am happy to note that 38 peer-reviewed papers are part of this volume covering various topics where Remote Sensing and GIS can be applied. The National and International Advisory Committee consisted of experts who have been recognised for their contribution.

I am sure the wealth of information contained in this volume will be useful for the Geomatics engineers who use a wide range of technologies for application in various fields like Civil Engineering, Computer Engineering and Software engineering covering a wide range of topics like land development and planning, satellite and information technologies, advanced surveying etc. The topics in Geoinformatics are interdisciplinary in nature. I am confident that this volume will be very useful and add to the knowledge in the interdisciplinary area of Geoinformatics. I convey my appreciation to the Organizing Secretaries of the Conference for the excellent work done.

Warangal, India

Prof. Bidyadhar Subudhi
Director

Preface

National Institute of Technology Warangal, the first among the chain of erstwhile Regional Engineering Colleges has a well established Department of Civil Engineering which runs an undergraduate and 8 Master degree programs besides Ph.D. One of the specializations is the Remote Sensing and GIS, started in the year 2000. Over the years, this programme has grown in stature and attracts many research projects.

A conference was organised to coincide with the superannuation of Prof. Deva Pratap, who initiated the starting of the Master degree program at NIT Warangal, and Shashi Mesapam, Keesara Venkatareddy and Manali Pal being the Organizing Secretaries. The conference attracted researchers from all parts of India as well as other countries. The conference had to be conducted in a virtual mode due to Covid. The papers covered various areas of application of Geomatics like water resources, environmental engineering, ecosystem management, structural health monitoring, transportation engineering, web GIS etc. The selected papers presented in the conference form the contents of this Lecture Note Series.

We are sure the contents of this volume will be useful for researchers working in the area of Remote Sensing and GIS.

Hanamkonda, India — Shashi Mesapam
Varanasi, India — Anurag Ohri
Blacksburg, USA — Venkataramana Sridhar
Bangkok, Thailand — Nitin Kumar Tripathi

Acknowledgements

A conference of this nature covering a wide area cannot be organized without the involvement of many individuals and organizations. We thank the Director and administration of NIT Warangal for all the infrastructure support. The conference had excellent national and international advisory committee for critically reviewing the papers and offering constructive suggestions for improving the quality of papers selected for the conference. Special mention must be made of IITT Navishkar I-Hub Foundation (IITTNiF) and GIS Monk whose financial support made the conference very successful.

Organizing Secretaries
Shashi Mesapam
Keesara Venkatareddy
Manali Pal

Contents

About the Editors

Prof. Shashi Mesapam is currently an Associate Professor at the Department of Civil Engineering, National Institute of Technology Warangal, India. He obtained his B.Tech. (Civil) from Osmania University, Hyderabad, and M.Tech. (Remote Sensing and Photogrammetric Engineering) and Ph.D. from the Indian Institute of Technology, Roorkee. His major areas of research interests include Photogrammetry, Unmanned Aerial Vehicles (UAV) and its Applications, Digital Image Processing, Remote Sensing, Advanced Surveying. He has published 26 papers in reputed international journals and 4 book chapters in reputed publications.

Prof. Anurag Ohri is currently an Associate Professor at the Department of Civil Engineering, Indian Institute of Technology (Banaras Hindu University), Varanasi, India. He obtained his B.Tech. (Civil) from Regional Engineering College, Kurukshetra, and M.Tech. (Remote Sensing and Photogrammetric Engineering) from the Indian Institute of Technology, Roorkee and Ph.D. from the Indian Institute of Technology (Banaras Hindu University). His major areas of research interests include Mapping, Development of GIS based Decision support systems, GIS application in Smart Cities, Land use planning. He has published 34 papers in reputed international journals and 3 book chapters in reputed publications.

Prof. Venkataramana Sridhar is currently an Associate Professor at the Biological Systems Engineering in Virginia Tech, Blacksburg, USA. He obtained his B.E. in Agricultural Engineering from Tamil Nadu Agricultural University, India and M.Eng. in Irrigation Engineering & Management from Asian Institute of Technology, Thailand and Ph.D. from Oklahoma State University, Stillwater, Oklahoma, USA. His major areas of research interests include Global change; urban systems and sustainability; agricultural water management; water resources systems; modeling; extreme events (floods and droughts); food-energy-water nexus; developing, implementing and evaluating earth system models; new hydrologic instrumentation, sensors, drones, databases, and model applications for use by federal, state, and private stakeholders for real-time operational applications; international activities. He has published 90 papers in reputed international journals and 6 book chapters in reputed publications.

Prof. Nitin Kumar Tripathi is currently a Professor at the Asian Institute of Technology, Thailand. He obtained his B.Tech. (Civil) from National Institute of Technology, Warangal, India, and M.Tech. (Remote Sensing) and Ph.D. from the Indian Institute of Technology, Kanpur. He has published 211 papers in reputed international journals, two books and 12 book chapters in reputed publications. He is currently Editor-in-chief of International Journal of Geoinformatics and Editorial Board Member of Int. Jour. of Applied earth Observation and Geoinformation (ITC Journal), Asian J. of Geoinformatics, Indian J. of Remote Sensing and Photogrammetry, Journal of Prince of Songkhla University, West Indian Journal of Civil Engineering, International Journal of Geoinformatics, Arabian Journal for Science and Engineering, International Journal of Remote Sensing—Taylor and Francis, International Journal of Imaging, J. of Chemistry and Environment, Geojournal—Springer, Disaster Advances, Natural Hazards, International Journal of Geographical Information Science.

Abbreviations

σ	Standard Deviation
%	Percent
°C	Degree Celsius
μ	Micro
2D	Two Dimensional
3D	Tridimensional
95PPU	95 Percent Prediction Uncertainty
ac	Acres
ADRF	Aerosol Direct Radiative Forcing
AHP	Analytic Hierarchy Process
AI	Aridity Index
ALPHA_BF	Base Flow Alpha Factor
ALPHA_BNK	Base Flow Alpha Factor For Bank Storage
AMD	Acid Mine Drainage
AMJ	April–June
ANN	Artificial Neural Network
AP	Andhra Pradesh
API	Application Programming Interface
APK	Android Package Kit
AQI	Air Quality Index
ASCAT	Advanced Scatterometer
ASMR	Advanced Microwave Scanning Radiometer-2
ASTER	Advanced Space Borne Thermal Emission and Reflection Radiometer
AT	Ambient Temperature
ATC	Air Traffic Control
AWBGT	Approximated Wet Bulb Globe Temperature
AWS	Annual Maximum Series
B	Blue
BBMP	Bruhat Bengaluru Mahanagara Palike
BMIC	Bengaluru Mysuru Infrastructure Corridor

BNU-ESM	Beijing Normal University Earth System Model
BOD	Biochemical Oxygen Demand
BSI	Bare Soil Index
BTA	Back Trajectory Analysis
BW	Bandwidth
C	Crop Management Factor
CA	Cellular Automata
Ca	Calcium
CaCO_3	Calcium Carbonate
CBD	Central Business District
CCME	Canadian Council Of Ministers of the Environment
CDD	Maximum Number of Consecutive Days When Daily Rainfall < 1 Mm
CGWB	Central Ground Water Board
CH_K2	Effective Hydraulic Conductivity in Main Channel Alluvium
CH_N2	Manning's N Value for the Main Channel
CI	Consistency Index
CIE	Commission for International Illumination
Cl	Chlorides
Cm	Centimeters
CMI	Crop Moisture Index
CMIP	Coupled Model Inter-Comparison Project
CMOS	Complementary Metal-Oxide-Semiconductor
CN	Curve Number
CNRM-CM5	Centre National for Meteorological Research Coupled Model Version 5
CO	Carbon Monoxide
Conc	Concentration
COVID	Corona Virus Disease
CP	Checkpoints
CPCB	Central Pollution Control Board
CR	Consistency Ratio
CRS	Coordinate Reference System
CRUTS	Climate Research Unit
CWC	Central Water Commission
CWD	Maximum Number of Consecutive Days When Rainfall > 1 Mm
CWT	Concentration Weighted Trajectory
D	Distance from Drainage Network
dB	Decibel
DEM	Digital Elevation Model
DIC	Digital Image Correlation
DN	Digital Number
DO	Dissolved Oxygen

DTM	Digital Terrain Model
EC	Electrical Conductivity
EDRIR	Earthquake Disaster Risk Index Report
EPCO	Plant Uptake Compensation Factor
EPSG	European Petroleum Survey Group
ERAinterim	European Reanalysis Interim
ERSCAT	European Remote Sensing Satellite Scatterometer
ESA	European Space Agency
ESCO	Soil Evaporation Compensation Factor
ESDAC	European Soil Data Center
ESDS	Earth Science Data System
ESRI	Environmental Systems Research Institute
ESSMI	Empirical Standardized Soil Moisture Index
ET	Evapotranspiration
ETM+	Enhanced Thematic Mapper Plus
EUFD	European Union Floods Directive
F	Flow Accumulation
FAO	Food and Agriculture Organization
FC	Field Capacity
FCC	False Colour Composite
FDM	Fused Deposition Modeling
Fig	Figure
FIM	Flood Inundation Mapping
FLOWA	Fuzzy Logic Ordered Weight Averaging
FR	Frequency Ratio
G	Green
G ratio	Green Ratio
GCC	Gnu Compiler Collection
GCM	General Circulation Models
GCP	Ground Control Point
GDVI	Green Difference Vegetation Index
GHG	Green House Gas
GHI	Global Horizontal Irradiance
GIMMS	Global Inventory Modeling and Mapping Studies
GIS	Geographic Information System
GNDVI	Green Normalized Difference Vegetation Index
GNSS	Global Navigation Satellite System
GPCC	Global Precipitation Climatology Centre
GPM	Ground Water Potential Mapping
GPS	Global Positioning System
GRD	Ground Range Detected
GRVI	Green Red Vegetation Index
GS	Ground Station
GSAVI	Green Soil Adjusted Vegetation Index
GSD	Ground Sample Distance

GUI	Graphical User Interface
GW	Ground Water
GW_DELAY	Groundwater Delay
GW_REVAP	Groundwater Revap Coefficient
GWDRVI	Green Wide Dynamic Range Vegetation Index
GWL	Ground Water Level
GWPI	Ground Water Potential Index
GWPZ	Ground Water Potential Zone
GWQMN	Threshold Depth of Water in the Shallow Aquifer Required For Return Flow (Mm)
H	Hue
H+	Hydrogen Ion
HCO_3	Bicarbonate
HD	High Definition
HEC	Hydrologic Engineering Centre
HEC-GeoRAS	Hydrologic Engineering Center's Geospatial River Analysis System
HEC-RAS	Hydrologic Engineering Center's River Analysis System
HI	Horizontal Irradiance
HMS	Hydrologic Modelling System
HR	Hazard Ranking
HRU	Hydrologic Response Unit
HWSD	Harmonized World Soil Database
HYSPLIT	Hybrid Single Particle Lagrangian Integrated Trajectory
IIASA	International Institute for Applied Systems Analysis
IMD	Indian Meteorological Department
IPCC	Intergovernmental Panel on Climate Change
IPSL-CM5A-MR	Institute Pierre-Simon Laplace Coupled Model Version 5A-Medium Resolution
IRDB	Irrigation Design and Research Board
ISC	Indian Standard Code
ISR	Impervious Surface Ratio
ISRIC	International Soil Reference and Information Centre
IT	Information Technology
IUCN	International Union for Conservation of Nature
JAS	July–August
JFM	January–March
K_c	Kappa Coefficient
K_{hist}	Kappa Histogram
kHz	Kilohertz
KIADB	Karnataka Industrial Areas Development Board
K_{loc}	Kappa Local
KM	Kilometers
KrRB	Krishna River Basin
KaRB	Karamana River Basin

KSB	Kijko-Sellevoll-Bayes
KSPCB	Kerala State Pollution Control Board
L	Length
Lat	Latitude
LAT Q	Lateral Flow
LC	Land Cover
Long	Longitude
LOS	Visible Line Of Sight
LR	Logistic Regression
LS	Slope Length and Slope Steepness Factor
LST	Land Surface Temperature
LULC	Land Use Land Cover
LWGNT	Surface Net Downward Longwave Flux
LWGNTCLN	Surface Net Downward Longwave Flux Assuming No Aerosol
LWTUP	Upwelling Longwave Flux at TOA
LWTUPCLN	Upwelling Longwave Flux at TOA Assuming No Aerosol
M	Meters
$M_{(max\verb|^|obs\ )}$	Observed Maximum Magnitude
Max	Maximum
MC	Markov Chain
Mc	Magnitude Completeness
MCDA	Multiple-Criteria Decision Analysis
MCDM	Multi Criteria Decision Making
Mg	Magnesium
Mg/L	Milligram per Liter
MGSAVI	Modified Green Soil Adjusted Vegetation Index
MHz	Megahertz
Min	Minimum
MK	Mann & Kendall
ml	Microliters
MLC	Maximum Likelihood Classification
M_{max}	Probable Maximum Earthquake Magnitudes
MOLUSCE	Modules for Land Use Change Evaluation
MSAVI	Second Modified Soil Adjusted Vegetation Index
MT	Metric Tons
MtP	Meteorological Parameters
mW	Milliwatt
Mw	Moment Magnitude
Na	Sodium
NASA	National Aeronautics and Space Administration
NBBSLUP	National Bureau of Soil Survey and Land Use Planning
NCR	Net Change Ratio
NDBI	Normalized Difference Built-Up Index
NDMA	National Disaster Management Authority

NDT	Non Destructive Testing
NDVI	Normalized Difference Vegetation Index
NDWI	Normalized Difference Water Index
NEX-GDDP	NASA Earth Exchange Global Daily Downscaled Climate Projections
NGT	National Green Tribunal
NHAI	National Highway Authority of India
NIR	Near Infra-Red
NLOS	Non Visible or Beyond Line Of Sight
NO_2	Nitrogen Dioxide
NPCM	Normalized Pairwise Comparison Matrix
NPI	National Pollution Index
NRSC	National Remote Sensing Centre
NSE	Nash-Sutcliffe Simulation Efficiency
NSF	National Sanitation Foundation
OA	Overall Accuracy
OBD	Over Burden Dump
OLI	Operational Land Imager
OND	October–December
OSM	Open Street Map
P	Support Practice Factor
PA	Producers Accuracy
PBIAS	Percentage Bias
PCM	Pairwise Comparison Matrix
PDSI	Palmer Drought Severity Index
PET	Potential Evapotranspiration
PLA	Polylactic Acid
Plat	Platinum
PM	Particulate Matter
PMP	Probable Maximum Precipitation
Ppm	Parts Per Million
PRCPTOT	Total Amount of Rainfall in Wet Days
PSCF	Potential Source Contribution Factor
PSO	Particle Swarm Optimisation
$PtCl^x{}_4$	Chloroplatinate Ion
PTFs	Pedotransfer Functions
PTL	Power Transmission Lines
PV	Photovoltaic
PVIP	Periyar Valley Irrigation Project
QGIS	Quantum Geographic Information System
QGIS	Quantum GIS
qp	Peak Discharge Per Sq. Km Area of Catchment
Qp	Peak Discharge of the Unit Hydrograph for the Catchment Area
QSWAT	QGIS Interface for Soil and Water Assessment Tool

r	Correlation Coefficient
R	Rainfall Erosivity Factor
Rd	Red
R10MM	Number of Days When RR > 10 mm. Count the Number of Days Where Rr_{ij} > 10 mm
R^2	Coefficient of Determination
R20MM	Number of Days When RR > 20 mm. Count the Number of Days Where Rr_{ij} > 20 mm
R95PTOT	Total Rainfall When RR > 95p
RCP	Representative Concentration Pathway
RECHARGE_DP	Deep Aquifer Percolation Factor
REVAPMN	Threshold Depth of Water for Revap or Percolation to Occur
RF	Random Forest
RGB	Red Green Blue
RH	Relative Humidity
RI	Rainfall Intensity
RI	Redness Index
RMSE	Root Mean Square Error
ROI	Region of Interest
RRMSE	Relative Root Mean Square Error
RS	Remote Sensing
RSR	Root Mean Square Error to Standard Deviation Ratio
RTK	Real Time Kinematic
RUSLE	Revised Universal Soil Loss Equation
RX1DAY	Monthly Maximum 1-Day Precipitation
RX5DAY	Monthly Maximum Consecutive 5-Day Precipitation
S	Slope
S	Saturation
S/cm	Simen Per Centimeter
SO_4	Sulphate
SAR	Synthetic Aperture Radar
SAVI	Soil Adjusted Vegetation Index
SCS	Soil Conservation Service
SDG	Sustainable Development Goal
SDR	Sediment Delivery Ratio
SED YIELD	Sediment Yield
SEZ	Special Economic Zone
SfM	Structure from Motion
SLEUTH	Slope Land Use Excluded Urban Transport Hillshade
SLR	Stepwise Linear Regression
SM	Soil Moisture
SMA	Soil Moisture Accounting
SMADI	Soil Moisture Agricultural Drought Index
SMAP	Soil Moisture Active Passive

SMDI	Soil Moisture Deficit Index
SMI	Soil Moisture Index
SMOS	Soil Moisture and Ocean Salinity
SMU	Soil Mapping Unit
SNAP	Sentinel Application Platform
SNR	Signal to Noise Ratio
SO_2	Sulphur Dioxide
SOC	Soil Organic Carbon
SOL_AWC	Available Water Capacity of the Soil Layer
SOL_BD	Moist Bulk Density Mm Layer
SOL_BD	Moist Bulk Density (G/Cm3)
SOL_K	Saturated Hydraulic Conductivity
SPEI	Standardized Precipitation Evapotranspiration Index
SPI	Standardized Precipitation Index
SPSS	Statistical Package for the Social Sciences
SR1 SR2 SR3 & SR4	Scenario 1 2 3 & 4
SSA	Seismic Study Area
SSM	Surface Soil Moisture
SSR	Surface Soil Roughness
STD	Standard Deviation
STL	Social and Travel Lockdown
SUFI 2	Sequential Uncertainty Fitting 2
SUH	Synthetic Unit Hydrograph
SUR Q	Surface Runoff
SURLAG	Surface Runoff Lag Coefficient
SWAT	Soil and Water Assessment Tool
SWAT CUP	SWAT Calibration and Uncertainty Programs
SWDI	Soil Water Deficit Index
SWGNT	Surface Net Downward Shortwave Flux
SWGNTCLN	Surface Net Downward Shortwave Flux Assuming No Aerosol
SWIR	Short Wave Infra Red
SWMM	Storm Water Management Model
SWTNT	Toa Net Downward Shortwave Flux
SWTNTCLN	TOA Net Downward Shortwave Flux Assuming No Aerosol
SY_{obd}	Observed Sediment Yield
SY_{pred}	Simulated Sediment Yield
T	Temperature
TA	Total Alkalinity
TB	Time Base of SUH
TC	Total Coliform
TCU	True Colour Unit
TDS	Total Dissolved Solids
TH	Total Hardness

TIN	Triangular Irregular Network
TIRS	Thermal Infrared Sensor
TM	Thematic Mapper
T_m	Peak Time of SUH
TNN	Monthly Minimum Value of Daily Minimum Temperature
TNX	Monthly Maximum Value of Daily Minimum Temperature
TOA	Top of Atmosphere
t_p	Basin Lag
TSA	Theil-Sen Approach
TWI	Topographic Wetness Index
TXN	Monthly Minimum Value of Daily Maximum Temperature
TXX	Monthly Maximum Value of Daily Maximum Temperature
UA	Users Accuracy
UAS	Unmanned Aerial System
UAV	Unmanned Aerial Vehicle
UER	Urban Expansion Rate
UGM	Urban Growth Model
UHI	Urban Heat Island
UR	Urbanization Rate
USDA	United States Department of Agriculture
USGS	United States Geological Survey
UTM	Universal Transverse Mercator
V	Value
VCI	Vegetation Condition Index
VES	Vertical Electrical Sounding
VIC	Variable Infiltration Capacity
VSWI	Vegetation Supply Water Index
W50	Width of SUH at 50% of Peak Discharge Ordinate Q_p in Hours
W75	Width of SUH at 75% of Peak Discharge Ordinate Q_p in Hours
WAD	World Atlas of Desertification
WAWQI	Weighted Arithmetic W_{qi}
WBGT	Wet Bulb Globe Temperature
WDVI	Weighted Difference Vegetation Index
W_f	Weightage Factor
WG	Western Ghats
WGS	World Geodetic System
WHO	World Health Organization
WMO	World Meteorological Organization
WOA	Weighted Overlay Analysis
WOE	Weight of Evidence
WP	Wilting Point
WQ	Water Quality
WQI	Water Quality Index

WR50	Half Width of SUH at 50% of Peak Discharge Ordinate Q_p in Hours
WR75	Half Width of SUH at 75% of Peak Discharge Ordinate Q_p in Hours
WRIS	Water Resource Information System
WRS	Worldwide Reference System
WS	Wind Speed
X_m	Highest Value in the Series
XML	Extensible Markup Language
X_n	Mean of N Annual Maximum Values
X_{n-m}	Mean of the Series Excluding the Highest Value
XS	Cross Section
YLCD	Yearly Land Cover Dynamic
Z_MK	Standardized MK-Test Statistic

Analyzing the Potential Application of Low-Cost Digital Image Correlation in Direct Shear Test

G. Alhakim, C. Nuñez-Temes, J. Ortiz-Sanz, and M. Arza-García

Abstract Nowadays, Digital Image Correlation (DIC) has become a frequently used optical technique for testing lab materials due to its nature of non-contact method, allowing for full-field displacements and strains to be accurately measured. The purpose of this study is to examine the potential employment of DIC in performing the standard direct shear test by using a modified box to observe and measure the shear properties of a soil sample. Accessible tools (e.g., a consumer grade DSLR camera) and DIC open-source software were employed in this study in order to monitor every portion of the speckled pattern during deformation and tracking the relative displacements. While it is often difficult to separate the relative contributions of individual error sources in any optical technique, we propose the use of two different validation methods for assessing the accuracy of DIC: the noise-floor and the direct comparison with a second trusted source, like transducers. The results of the conducted study demonstrate that the DIC technique implemented on a properly prepared direct shear laboratory setup opens up new possibilities for the effective and accurate analysis of deformations in soil materials under direct shear loading conditions. The calculations of the noise floor of the setup and speckled pattern in terms of the mean and distribution of the displacements showed validated results with STD of 0.001 and 0.0012 mm for the horizontal and vertical planar components, respectively. The displacements measured by DIC showed good agreement with the results of the transducer with an average error of 0.1 mm.

Keywords Direct shear test · DIC analysis · Displacement measurement · NDT

G. Alhakim (✉) · C. Nuñez-Temes · J. Ortiz-Sanz · M. Arza-García
Civil and Geomatics Research Group, Department of Agroforestry Engineering, University of Santiago de Compostela, Santiago, Spain
e-mail: g.hakim@bau.edu.lb

G. Alhakim
Civil and Environmental Engineering Department, Faculty of Engineering, Beirut Arab University, Beirut, Lebanon

S. Mesapam et al. (eds.), *Developments and Applications of Geomatics*,
Lecture Notes in Civil Engineering 450, https://doi.org/10.1007/978-981-99-8568-5_1

1 Introduction

In recent years, Digital image correlation (DIC) has become one of the preferred optical techniques for the analysis of close-range displacements in several lab and in-field experiments, being able to capture the shape, motion, and deformation of object surfaces. Since the development of these DIC methods over the past decades, numerous applications have been found in many fields and areas of research, due to its ease of use. Hence, this technique has found a particularly interesting application niche in those fields related to civil engineering.

The basic principle of DIC is to track a speckle pattern in a sequence of images and to calculate the displacements of small portions of this pattern (often called subsets) between one reference image and the other (deformed) images. The variations of coordinates between the original and deformed subset centers provide the required displacement vector of the targeted point. Similarly, the full-field deformation of other interrogated points could be acquired. For this purpose, DIC usually requires an artificial speckle pattern to resolve unique issues [1]. Nonetheless, the pattern can also sometimes be naturally present over the surface of some materials (e.g., rocks, sand, etc.).

In general, there are now multiple software solutions, both commercial and open source, to perform the correlation between the images. Among others, we can find commercial systems like Aramis (GOM) or VIC-3D (Correlated Solutions), that are normally provided with their own specialized hardware and optical components. As the use of DIC becomes more and more widespread, diverse open-source projects are also emerging (e.g., nCorr [2], py2DIC [3], etc.) making this technique more accessible, even for small companies and laboratories with more limited resources. At a level of hardware, also industrial high-speed cameras have proven to be replaceable—at low cost—by consumer grade cameras in certain experimental setups where the frame rate is not a decisive issue [4]. The affordability of the approach and the simplicity of its implementation have democratized to some extent the use of DIC, bringing it closer to all practitioners.

DIC is currently considered a simple but reliable technique for analyzing surface displacements and deformations. However, the analysis of the results and their accurate assessment can be technically challenging. The main problem is a general lack of control over the final quality of the output, as the users are sometimes more fascinated by the detail of the full-field maps rather than aware of the metric quality of the results obtained. It is important to remark that DIC measurements, as many other optical techniques, are affected by different types of errors. Among others, the results can be affected by the stationary noise from camera sensors, errors related to the illumination or temperature, errors associated with speckle pattern, errors associated with the processing, external biases (e.g., vibrations), etc. [5, 6]. Therefore, the accuracy of every experiment requires careful verification.

1.1 DIC Applications in Lab Testing of Materials

The experimental technique of imaging correlation has gained widespread acceptance as a reliable tool for strain measurements. Thus, DIC has been appealing to researchers in various engineering applications as a non-destructive testing (NDT). Many studies have examined the use of the DIC technique to analyze the concrete behavior, such as the distribution of deformation and crack propagation of concrete [7], quantification of the fracture properties [8] and fatigue behavior [9] of reinforced concrete beams. Besides, the DIC optical method was employed to assess the behavior of road materials [10–12].

Furthermore, geotechnical engineering investigation relies greatly on DIC practices to determine subpixel displacements in the soil, through which strain is estimated [13]. Plé, Tourabi and Abuaisha [14] have investigated the strain deformation during a direct tensile test performed on a clayey soil by applying 3-D DIC technique. They stated that this method could be adapted for the strain determination of the cap cover in landfills composed of compacted clay. A modified consolidation mold has been developed to monitor the micro-structure behavior of unsaturated soil with axial drainage conditions. By using this half mold oedometer apparatus, Liu et al. [15] studied the deformation field of silty clay soil by applying digital image analysis. They declared the importance of this study in terms of understanding the correlation between micro and macro mechanical properties of the soil. Ko et al. [16] conducted an experiment of a small-scale retaining wall by reproducing the collapse behavior of the structure and measured the deformation and displacement of the whole surface of the wall by using 3D-DIC. Tong and Yoo [17] discussed the application of DIC technology on geotechnical small-scale models such as a retaining wall, trapdoor, shallow footing, and tensile test on geogrid. They revealed the effectiveness of DIC in monitoring the deformation and strain field during these laboratory tests.

1.2 Direct Shear Test

The direct shear test is one of the oldest experimental procedures implemented in geotechnical engineering practice, and it is the most widely used geotechnical shear device due to its simplicity. This experimental procedure is conducted in order to determine the shear strength and shear parameters of soil materials. The accurate determination of these parameters represents a key issue in the design of various structures, e.g., retaining walls, earth buildings, dams, and roads, as well as the design of foundations beneath any architectural and/or engineering structure. However, one of the demerits of the direct shear test could be the non-uniform distributions of stress and strain on the failure plane.

Accordingly, numerical methods have been employed to analyze the details of stress and strain occurrence within a shear box, that would be difficult to measure in the experimental study. Dirgelienė, Skuodis and Grigusevičius [18] carried out experimental and numerical investigations of the direct shear test performed under constant vertical stress and constant sample volume. The results of the finite element method showed that the vertical stress and displacements were non-uniformly distributed in the sample in both conditions. Zhang and Thornton [19] simulated the direct shear test by using the discrete element method and illustrated the heterogeneous distributions of stress and strain. In addition, they demonstrated that the shear strain as well as the dilation concentrated in the mid-height of the specimens (within the shear zone). To study the soil behavior at the microscopic level, Yan [20] presented a 3-D numerical model of granular soil with elongated particles in a direct shear test. It was observed that a localized dilative shear zone was revealed along the failure plane and the change in particle orientation was clearly noticed.

While these non-uniform distributions of stress and strain can be numerically modelled, the employment of a full-field measurement NDT method like DIC could be very useful for tracking experimentally the changes in displacements on the lateral surface of the sheared samples and for validating the models [21]. The main limitation for applying DIC in the direct shear test is that the mold used in the test apparatus is a metal closed box, which makes it impossible to monitor the real behavior of the soil. Kong, Cheng, and Hua [22] applied digital image technique to direct shear test by employing a modified shear box and determined the displacement and strain fields as well as the particle orientation. They concluded that the maximum shear strain occurred at the interface between the upper and lower shear boxes and the formation of shear band could be clearly detected. However, in their research they did not consider any method to validate the accuracy of DIC.

The review of the mentioned studies enlightens the benefits of DIC application in the direct shear test to monitor the strain field and displacement instead of assuming uniform distribution of stress and strain during shearing. Despite this, the usage of the DIC technique in the direct shear test of soil has not been fully investigated yet, especially when it comes to quantify the precision of this technology in this experimental test. Hence, the main objective of this research is to study the potential application of DIC in conducting the direct shear test on soil. Accordingly, a modified shear box and mold were designed for this purpose and accessible tools (e.g., a consumer grade digital single-lens reflex (DSLR) camera and open-source software) were employed. The relative contributions of individual error sources are hardly separated in any optical practice. Therefore, we suggest the use of two different validation methods to quantify the accuracy of DIC: the noise-floor, and the direct comparison with a conventional contact measurement device.

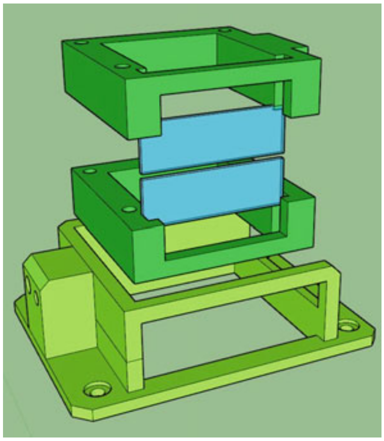

Fig. 1 Shear mold and box in 3-D model

2 Materials and Method

2.1 Shear Mold

In order to monitor the soil grains displacement and the deformation during shearing, the original shear box must be modified by cutting one of the sides of the upper and lower molds. For experimental purposes, and to prevent the damage of the original metal mold, a new cost-effective one was produced by applying Fused Deposition Modeling (FDM) printing. A 3-D printed mold was manufactured with a Prusa i3 (BQ, Spain) 3-D printer by using a bioplastic filament material, namely, Polylactic Acid (PLA). The original dimensions of the shear box (60 × 60 mm) were maintained. Moreover, the open sides of the upper and lower boxes were replaced with two plexiglass plates of 3 mm thickness, as illustrated in Fig. 1.

2.2 2D-DIC Fundamentals

To be able to analyze displacements with 2D-DIC in the image series, the first stage consists in selecting a subset or portion of the speckled pattern to be tracked. The subset size should be chosen in a way that allows to distinguish every subset in the region of interest from all other subsets. There is no one-size-fits-all rule in this sense, but it is commonly accepted between DIC practitioners to choose a subset size that allows facets containing at least 3 speckles. Larger subsets typically result in lower displacement noise, but often at the cost of increased spatial smoothing [23]. A process of image correlation is performed to detect homologous subsets between the reference image and the deformed ones.

As illustrated in Fig. 2, the coordinates of the central point of every initial subset can be mapped in the target subset by using the computed image displacement and first-order shape functions, representing translations, rotations, normal and shear strains (Eqs. 1 and 2).

$$\varsigma 1 = \mathrm{u} + (\partial \mathrm{u} \partial \mathrm{x})\mathrm{dx} + (\partial \mathrm{u} \partial \mathrm{v})\mathrm{dy} \tag{1}$$

$$\eta 1 = \mathrm{v} + (\partial \mathrm{v} \partial \mathrm{x})\mathrm{dx} + (\partial \mathrm{v} \partial \mathrm{y})\mathrm{dy} \tag{2}$$

where ζ1 and η1 are the displacements of the subset; u and v represent the translations; ∂u/∂x and ∂v/∂y represent the normal strains; ∂u/∂y and ∂v/∂x represent the shear strains; and dx and dy represent the distances from the subset center to an arbitrary point within the same subset in the x and y directions, respectively.

As DIC software works with pixel units, the displacement maps resulting from processing all the points of interest do not have an inherent scale. For this reason, DIC requires a calibration procedure to establish the image scale, relating pixel units with real units (what can be even done with a simple known distance). However, at the same time, the calibration procedure can be also used to correct for lens distortions if a calibration plate is used. In this study, we performed the 2D-DIC calibration by taking images of a special calibration plate (i.e., symmetric dot grid target) prior to the experiments. By tracking the displacements of the points of the grid in along the images of the plate, the parameters of the camera can be calibrated. If the intrinsic and extrinsic parameters of a 2D, single camera system are calibrated, then an out-of-plane tilt of the test piece can be determined and corrected. In any case, when only one camera is used for DIC (2D-DIC) is crucial to ensure that the translation remain strictly perpendicular to the optical axis; otherwise, false displacements due to out-of-plane motion will be produced.

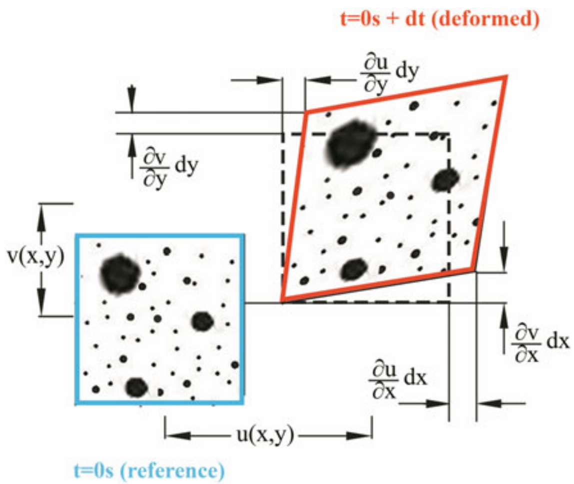

Fig. 2 Schematic illustration of the basic principles in 2-D DIC